Caspase-1–mediated pathway promotes generation of thromboinflammatory microparticles

Andrea S. Rothmeier,[1] Patrizia Marchese,[2] Brian G. Petrich,[3] Christian Furlan-Freguia,[1] Mark H. Ginsberg,[4] Zaverio M. Ruggeri,[2] and Wolfram Ruf[1,5]

[1]Department of Immunology and Microbial Science and [2]Department of Molecular and Experimental Medicine, The Scripps Research Institute, La Jolla, California, USA. [3]School of Medicine, Emory University, Atlanta, Georgia, USA. [4]Department of Medicine, UCSD, La Jolla, California, USA. [5]Center for Thrombosis and Hemostasis, University Medical Center Mainz, Mainz, Germany.

Extracellular ATP is a signal of tissue damage and induces macrophage responses that amplify inflammation and coagulation. Here we demonstrate that ATP signaling through macrophage P2X7 receptors uncouples the thioredoxin (TRX)/TRX reductase (TRXR) system and activates the inflammasome through endosome-generated ROS. TRXR and inflammasome activity promoted filopodia formation, cellular release of reduced TRX, and generation of extracellular thiol pathway–dependent, procoagulant microparticles (MPs). Additionally, inflammasome-induced activation of an intracellular caspase-1/calpain cysteine protease cascade degraded filamin, thereby severing bonds between the cytoskeleton and tissue factor (TF), the cell surface receptor responsible for coagulation activation. This cascade enabled TF trafficking from rafts to filopodia and ultimately onto phosphatidylserine-positive, highly procoagulant MPs. Furthermore, caspase-1 specifically facilitated cell surface actin exposure, which was required for the final release of highly procoagulant MPs from filopodia. Together, the results of this study delineate a thromboinflammatory pathway and suggest that components of this pathway have potential as pharmacological targets to simultaneously attenuate inflammation and innate immune cell–induced thrombosis.

Introduction

Atherosclerosis and its thrombo-occlusive complications remain a major cause of morbidity and mortality from cardiovascular diseases worldwide. Atherosclerotic plaques are complex inflammatory lesions with variable stability that upon rupture can cause acute thrombosis, vessel occlusion, and infarct (1). A major source for inflammatory and prothrombotic mediators are atherosclerotic plaque macrophages that express the proinflammatory cytokine IL-1β (2, 3) and tissue factor (TF) (4), which initiates the coagulation cascade (5).

A large body of evidence indicates an important role for IL-1β in the pathogenesis and progression of atherosclerosis (6). Endogenous or exogenous ligands for Toll-like receptors (TLRs), particularly TLR4 in atherosclerosis (7), specifically induce macrophage synthesis of the inactive pro-form of IL-1β. Secondary signals, including cholesterol crystals, a hallmark of atherosclerotic lesions (8), are required for assembly of the functional inflammasome multiprotein complex of NOD-like receptor family, pyrin containing 3 (NLRP3), apoptosis-associated speck-like protein containing a CARD (ASC), and procaspase-1. Activation of caspase-1 in this complex leads to cytokine maturation and release (9), although the final steps of IL-1β secretion are poorly understood (10).

Thrombosis is dependent on TF that is also induced by endogenous TLR ligands promoting atherosclerosis (11). Analogous to cytokine processing, TF is kept in an inactive form on the surface of myelomonocytic cells and requires additional signals to become fully procoagulant (12, 13). Activation of TF prothrombotic function is a thiol-disulfide exchange–dependent and protein disulfide isomerase–regulated (PDI-regulated) process (14) that occurs following outer membrane leaflet exposure of procoagulant phosphatidylserine (PS) (13, 15) and may involve other cell surface redox partners in the context of thrombosis (16, 17).

P2X7 receptor (P2RX7 in mice) activation has well-established roles in proinflammatory effects of macrophages (18). The purinergic receptor responds to extracellular ATP released from inflamed or damaged cells and is one of several signals that can activate the inflammasome and caspase-1–mediated processing of IL-1β (19). P2RX7 signaling also induces activation of cell surface TF and release of procoagulant TF-bearing microparticles (MPs) (12, 20). ATP promotes experimental thrombosis through platelet and neutrophil P2RX1 activation (21, 22) and P2RX7 signaling in mice (12). Since new biosensors have revealed the presence of high pericellular concentrations of ATP in inflammatory conditions in vivo (23), the presence of P2RX7 on macrophages in human atherosclerotic plaques (24) may indicate roles in the pathogenesis of arterial thrombotic complications of atherosclerosis.

P2RX7-mediated activation of macrophage TF procoagulant function specifically leads to extracellular thiol-disulfide exchange–dependent generation of procoagulant MPs carrying TF and integrin β1 as well as P-selectin glycoprotein ligand 1 (PSGL1), a major counterligand for platelet P-selectin in thrombotic vessel occlusion (25, 26). Indeed, atherosclerotic lesions accumulate large amounts of MPs that may support thrombus propagation upon plaque rupture (27). Although emerging evidence indicates that MP-incorporated proteins vary depending on the releasing stimulus (28, 29), little is known about the cellular mechanisms that determine MP composition and biological function.

Conflict of interest: The authors have declared that no conflict of interest exists.
Submitted: October 2, 2014; **Accepted:** January 9, 2015.
Reference information: *J Clin Invest*. 2015;125(4):1471–1484. doi:10.1172/JCI79329.

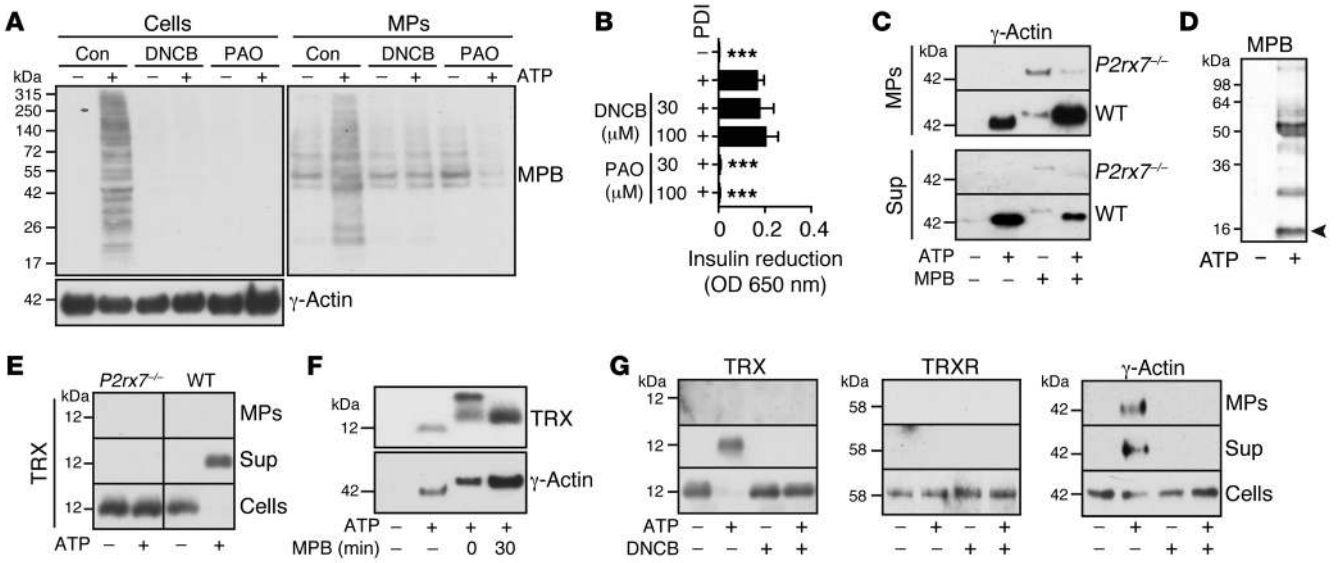

Figure 1. P2X7 receptor activation induces TRXR-dependent extracellular thiol-disulfide exchange. (**A**) Effects of DNCB or PAO on ATP-induced exposure of solvent-accessible free thiols on the cell or MP surface were measured by thiol labeling with MPB and detected by streptavidin blotting. Detection of cellular γ-actin by Western blotting served as loading control. (**B**) Inhibition of PDI reductase activity measured by reduction of insulin by PDI with PAO or DNCB added at the indicated micromolar concentrations; mean ± SD, ***$P < 0.001$, ANOVA (Bonferroni). (**C**) Western blotting for γ-actin in MPs and MP-depleted supernatant from WT and *P2rx7*$^{-/-}$ macrophages stimulated with ATP in the presence or absence of MPB. (**D**) Streptavidin blot for thiol labeling with MPB detects a prominent protein band (arrowhead) of approximately 12 kDa – consistent with the molecular weight of TRX in the MP-free supernatant of ATP-stimulated cells. (**E**) Western blotting for TRX in cells, MPs, and MP-free supernatant of *P2rx7*$^{-/-}$ and WT macrophages. (**F**) MPB modification of free thiol groups in TRX alters electrophoretic mobility. MPB was added at the beginning of (0 minutes) or 30 minutes after ATP stimulation. Proteins were detected by Western blot. (**G**) Effect of DNCB on ATP-induced release of γ-actin, TRX, or TRXR determined by Western blotting. Cell lysates were diluted 1:10 for γ-actin blot.

Working with the hypothesis that MP protein cargo is a unique fingerprint of underlying release mechanisms, we focused on defining the MP proteome susceptible to reduction during MP generation following prothrombotic P2RX7 activation. Here, we identify the thioredoxin (TRX)/TRX reductase (TRXR) system as a common upstream regulator for both procoagulant and proinflammatory responses of macrophages; and elucidate key steps of this pathway that ultimately triggers MP release through an unexpected function of caspase-1–dependent actin remodeling in primary cells.

Results

P2RX7 activation induces extracellular reductive changes dependent on TRXR. The mechanism through which P2RX7 activation by ATP leads to reductive changes in the extracellular proteome of macrophages and on released MPs (12), as detected by thiol labeling with the extracellular, water-soluble probe 3-(*N*-maleimido-propionyl)-biocytin (MPB) (Figure 1A), has remained unexplained to date. By using biotinylated PEG-maleimide with a membrane-impermeable molecular weight of 10 kDa, we confirmed that thiol labeling occurred extracellularly (Supplemental Figure 1A; supplemental material available online with this article; doi:10.1172/JCI79329DS1). Consistent with thiol-isomerase dependence of TF^{+} MP release, the vicinal thiol blocker phenylarsine oxide (PAO) prevented the appearance of solvent-accessible free thiols on the cell surface and on MPs (12). Although PAO might have blocked labeling of a variety of cell surface proteins carrying vicinal thiols, ATP-stimulated cells pretreated with 2,4-dinitrochlorobenzene (DNCB) also had markedly reduced cell surface free thiols. These data were surprising, since DNCB, unlike PAO, is not an inhibitor of reducing vicinal thiol groups, as confirmed for the reductive function of the thiol-isomerase PDI in an insulin reductase assay (Figure 1B).

As used here at low micromolar concentrations, DNCB rapidly and specifically inactivates the TRXR catalytic selenocysteine residue even in the presence of physiological intracellular concentrations (mM) of reduced glutathione (GSH), but not the vicinal thiols of TRXR required for NADPH oxidase activity (30). Prolonged inhibition of TRXR is known to affect the cellular redox equilibrium by depleting GSH. However, we measured only minimally lower levels of GSH after 20 minutes of ATP stimulation in DNCB-treated macrophages (85% ± 10% of ATP-stimulated controls). These results suggested that the effects of DNCB resulted primarily from TRXR inhibition and not global changes in redox equilibrium.

The search for potential MP redox-regulated proteins by mass spectrometry did not identify proteins with vicinal thiols as potential downstream targets of TRXR. Rather, a major 54-kDa MP-associated thiol-labeled protein was identified as γ-actin. Western blotting showed that γ-actin was markedly increased in the MP fraction after ATP stimulation as well as released into the MP-depleted supernatant (Figure 1C). Thus, potential markers for the MP release mechanism may also be found in the cell supernatant. MPB labeling altered γ-actin electrophoretic mobility, suggesting that at least 1 of the 6 cysteine residues (31) was reduced and solvent exposed in the extracellular space (Figure

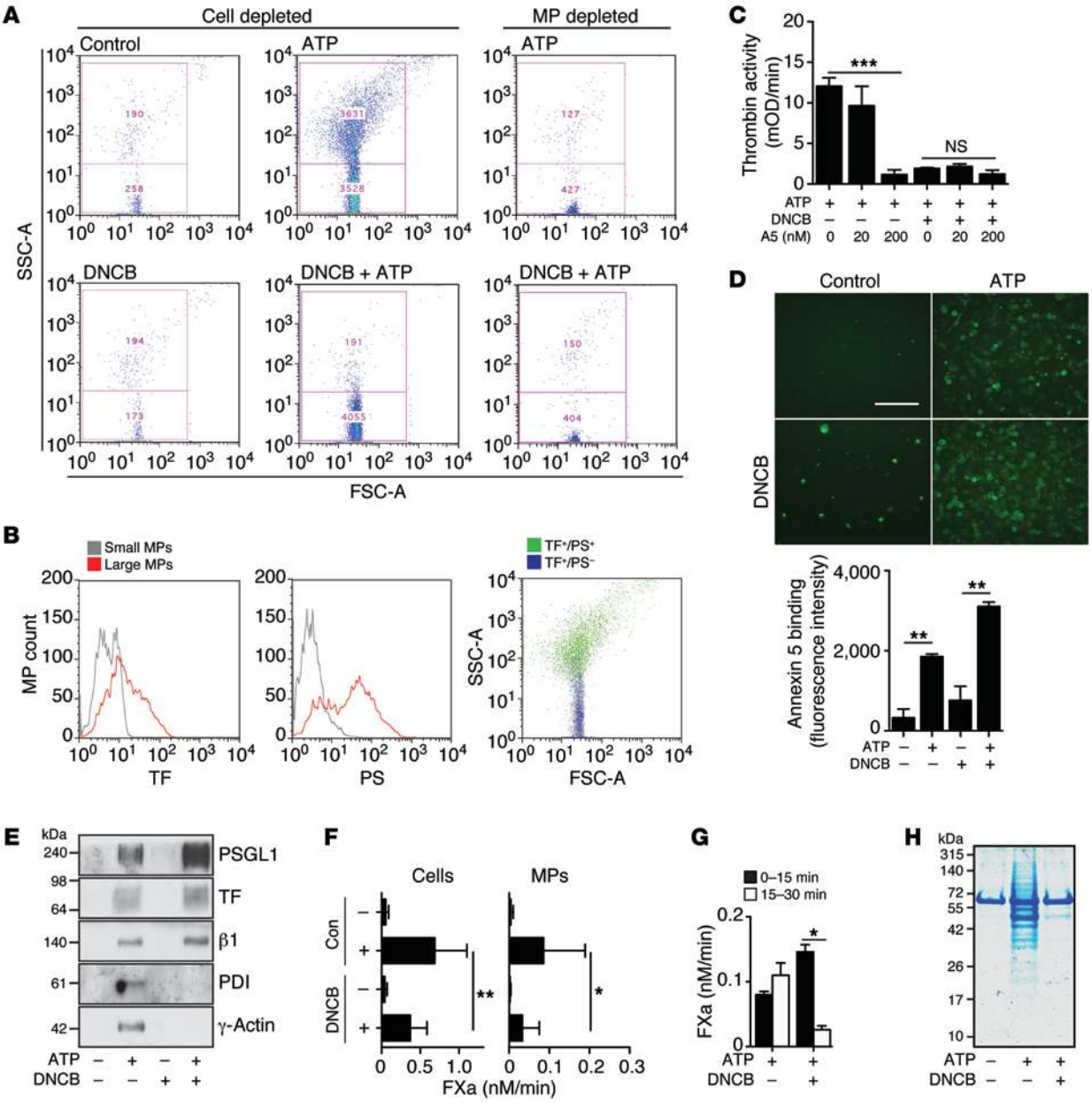

Figure 2. TRXR is required for the release of highly procoagulant MPs downstream of P2RX7 activation. (**A**) FACS analysis of large high side scatter (SSC) and small low SSC MPs released from control and ATP-stimulated TFKI macrophages with or without DNCB treatment. MP-depleted cell supernatants of ATP-stimulated cells were analyzed as an additional control. FSC, forward scatter. (**B**) Detection of TF and PS on ATP-induced MP populations. (**C**) PS-dependent prothrombinase activity of macrophage MPs generated with or without DNCB. PS dependence was confirmed by blockade with annexin 5 (A5); mean ± SD, $n = 3$, $^{***}P < 0.001$, ANOVA (Bonferroni). (**D**) Annexin 5 staining of ATP-stimulated WT cells after 30 minutes with and without DNCB treatment showed that blocking TRXR did not prevent cell surface PS exposure; scale bar: 100 μm; mean ± SD, $n = 3$, $^{**}P < 0.01$, t test. (**E**) Detection of PSGL1, TF, integrin β1, PDI, and γ-actin on ATP-induced MPs from control and DNCB-treated TFKI macrophages by Western blot. (**F**) Effect of DNCB on TF activity on cells and MPs from control (–) and ATP-stimulated (+) cells measured by FXa generation assay; mean ± SD, $n = 13$, $^{*}P < 0.05$, $^{**}P < 0.01$, ANOVA (Bonferroni). (**G**) TF activity on MPs collected 0–15 minutes and 15–30 minutes following ATP stimulation of control and DNCB-treated cells; mean ± SD, $n = 3$, $^{*}P < 0.05$, ANOVA (Bonferroni). (**H**) Coomassie blue–stained gels of MP-depleted supernatants of control and ATP-stimulated TFKI macrophages with or without DNCB treatment. Six prominent protein bands were identified by mass spectrometry (see Supplemental Table 1 for results).

1C). Notably, actin is known to interact with TRX, the substrate of TRXR (32). The MP-depleted supernatant of ATP-stimulated macrophages showed a thiol-labeled protein of 12 kDa, consistent with the molecular mass of TRX (Figure 1D). Indeed, ATP stimulation of macrophages led to a P2RX7-dependent complete release of cellular TRX (Figure 1E).

TRX contains 2 vicinal and 4 noncatalytic cysteine residues (33). When free thiols were labeled with MPB (MW = 523) during (MPB added $t = 0$ minutes) or after ($t = 30$ minutes) MP release, TRX, but not γ-actin, showed differences in mobility (Figure 1F). The increased thiol content evidenced by the larger molecular mass of TRX in samples labeled continuously during the reaction

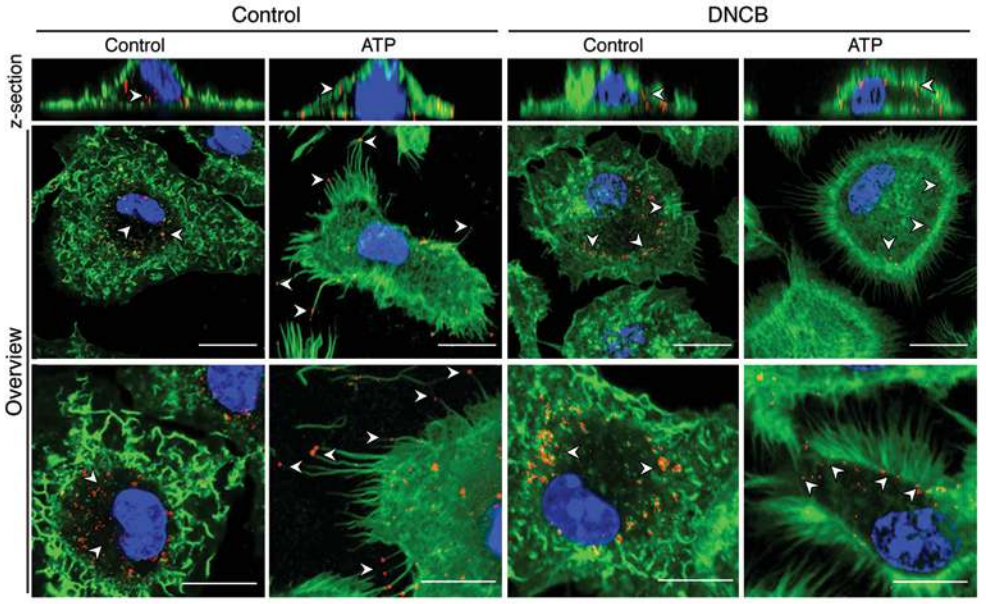

Figure 3. P2RX7 activation induces TF trafficking to filopodia dependent on TRXR. Tracking of cell surface TF labeled with anti–TF–Alexa 647 conjugate (red) for 10 minutes prior to agonist stimulation with ATP for 20 minutes in the presence or absence of DNCB added 30 minutes before TF staining. TFKI macrophages were counterstained with phalloidin–Alexa 488 and Hoechst stain to visualize F-actin (green) and nuclei (blue), respectively. Representative overviews with z-section and views at higher magnification are shown (scale bars: 10 μm). White arrowheads indicate TF localizations.

indicated that TRX was initially released in a more reduced form and then became oxidized in the extracellular space. Although TRX release required functional TRXR, TRXR was not released from P2RX7-stimulated cells (Figure 1G), indicating uncoupling of the TRXR/TRX system. Moreover, TRX secretion and extracellular MPB labeling occurred with remarkably similar kinetics (Supplemental Figure 1B), and inhibiting TRX directly following its release with the oxidizer PX-12 effectively diminished MPB labeling of cell surface proteins (Supplemental Figure 1C). Taken together, these data show that the reductive function of TRXR is required for the release of reduced TRX, which in turn promotes exposure of extracellular thiol groups following P2RX7 activation.

P2RX7-induced release of highly procoagulant MPs is dependent on TRXR. We then evaluated by flow cytometry how blockade of the TRXR system with DNCB influenced the thiol-disulfide exchange–dependent release of MPs. We used macrophages expressing human TF (TF knock-in [TFKI] mice) (34) to facilitate TF detection by FACS and confirmed that these cells were indistinguishable from macrophages expressing mouse TF in P2RX7-dependent MP release and response to inhibitor treatment (Supplemental Figure 2, A–D).

ATP stimulation generated a population of large MPs (Figure 2A) with sizes ranging from 200 to 500 nm (Supplemental Figure 2, E and F). These MPs were no longer generated from DNCB-treated cells, whereas smaller vesicles were still released (Figure 2A). Collecting MPs from control and DCNB-treated cells by centrifugation at different speeds further supported different physical properties of these MPs (Supplemental Figure 3A). Detection of procoagulant PS by lactadherin (35) and of TF by a specific mAb (Supplemental Figure 3B) showed that only the large MP population carried both PS and TF, whereas the smaller MPs released from DNCB-treated cells incorporated TF, but little PS (Figure 2B). Accordingly, MPs released from DNCB-treated cells had low procoagulant activity in a prothrombinase assay, whereas high prothrombinase activity of MPs generated in the absence of DNCB was confirmed to be dependent on functional PS by blockade with annexin 5 (Figure 2C). Based on these findings, we defined the large MP population carrying TF and PS as highly procoagulant MPs. Notably, blocking TRXR did not prevent PS exposure detected by annexin 5 staining on the cell surface (Figure 2D), demonstrating that outer leaflet presence of PS alone does not promote highly procoagulant MP generation. To exclude compound-specific effects of DNCB, we reproduced the results of key experiments with relevant concentrations of another well-established inhibitor of TRXR, auranofin (36), as well as PX-12, which at high concentrations inhibits the TRX/TRXR system by a distinct mechanism not primarily targeting the catalytic selenocysteine residue of TRXR (37) (Supplemental Figure 4).

Further characterization of MPs released from TRXR-blocked cells (Figure 2C and Supplemental Figure 2A) confirmed the presence of membrane receptors — TF, PSGL1, and integrin β1 — but not of the TRX-interacting components PDI and γ-actin. Control experiments showed that ROS production, which was not blocked by DNCB, was responsible for the release of membrane receptors on MPs (Supplemental Figure 5, A and B). Despite similar TF antigen levels, TF-FVIIa–mediated FX activation was significantly diminished on MPs from DNCB-treated cells (Figure 2D and Supplemental Figure 2B), consistent with reduced content of PS (Figure 2B). TF-specific activity in WT macrophages, based on normalization to TF antigen, was markedly reduced by DNCB to 31% ± 13% ($n = 14$, $P < 0.0001$) of uninhibited control, demonstrating the formation of MPs with low TF procoagulant activity.

While macrophage TF procoagulant activity is high when analyzed with suspended cells (Supplemental Figure 5C), consistent with previous results (20), TF on adherent cells has low coagulant activity and requires P2RX7 activation. Rapid cellular TF activation and MP TF activity early after ATP stimulation were minimally inhibited by DNCB. However, TF activity on MPs collected after 15 minutes of ATP stimulation required a functional TRXR system (Figure 2E and Supplemental Figure 2C). These data indicated that activation of the TRXR pathway specifically promoted sequential cellular events that generated highly procoag-

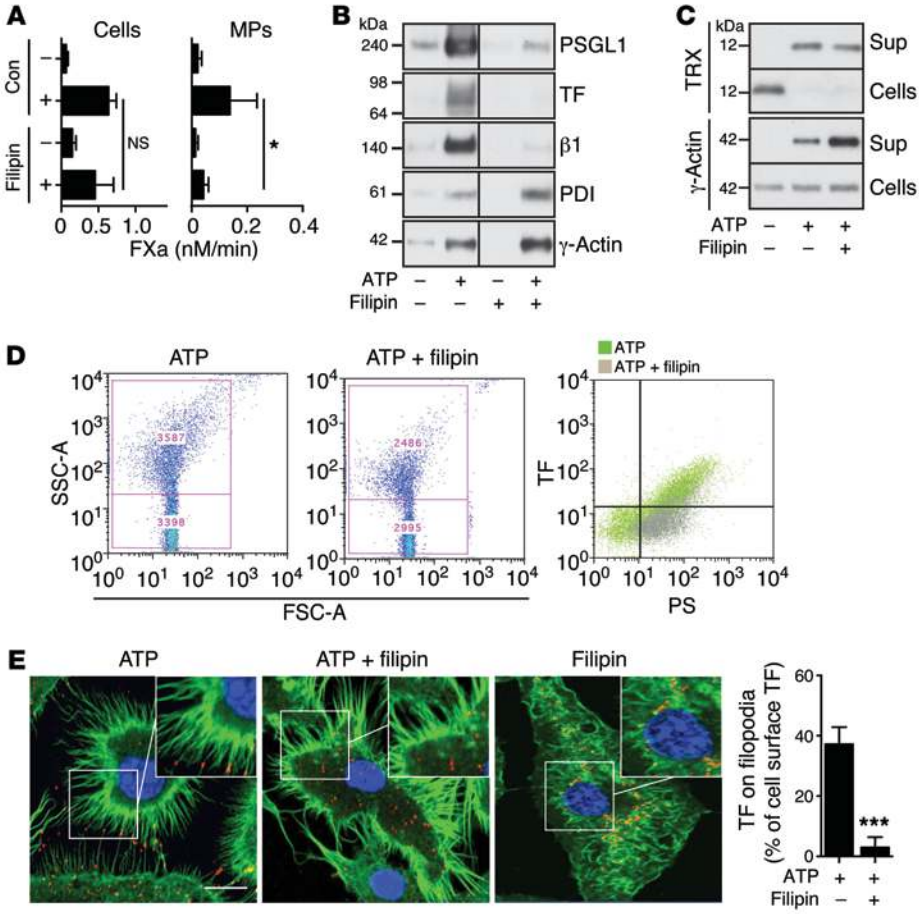

Figure 4. TF and integrin β1 incorporation into MPs requires functional lipid raft domains. (**A**) Effect of filipin treatment on TF cell surface and MP activity with control and ATP-stimulated TFKI macrophages; mean ± SD, $n = 7$, $^*P < 0.05$, ANOVA (Bonferroni). (**B**) Effect of filipin on MP incorporation of PSGL1, TF, integrin β1, PDI, and γ-actin detected by Western blotting. (**C**) Effect of filipin treatment on the release of TRX and γ-actin into the MP-depleted supernatants detected by Western blotting. (**D**) FACS analysis of MPs released from ATP-stimulated TFKI macrophages with or without filipin pretreatment. Event counts are displayed in the indicated gates of large and small MPs. Right panel: Scatter plot of TF and PS staining for MPs from ATP-stimulated cells with (gray) or without (green) filipin pretreatment. (**E**) Effects of filipin on filopodia formation and localization of TF (red) in control and ATP-activated macrophages. Cells were counterstained after permeabilization for F-actin (green) and nuclei (blue); scale bar: 10 μm. Right panel: Quantification of TF distribution on filopodia versus the cell body; mean ± SD, $n = 6$, $^{***}P < 0.001$, *t* test.

ulant MPs for extended time periods. This pathway also released various soluble proteins into the extracellular space (Figure 2F), including cytoskeleton-associated proteins and annexins 1 and 5 (Supplemental Table 1), which are known to interact with the MP components actin and PS (38, 39).

TRXR is required for lipid raft–dependent translocation of TF onto filopodia. To clarify how membrane receptors are incorporated into highly procoagulant MPs, we tracked TF during the course of stimulation with antibodies (40) on TFKI macrophages. Control experiments excluded antibody-induced TF internalization following specific staining of the human protein, and demonstrated that the specifically labeled cell surface pool of TF, and not potential Golgi-mobilized TF (41), became activated and released on MPs (Supplemental Figure 6, A–C).

ATP stimulation promoted TF translocation onto filopodia (Figure 3) that formed concomitantly with measurable TF activity and release on MPs (Supplemental Figure 7, A–D). Blocking TRXR markedly reduced the length of filopodia in ATP-stimulated cells, and, most significantly, TF accumulated on the cell surface in the distal cellular cortex but was not further transported onto extending filopodia (Figure 3 and 3-dimensional reconstructions in Supplemental Videos 1–4). Confirming the requirement for filopodia formation to generate highly procoagulant MPs, we showed that pretreatment with the membrane-permeable actin filament stabilizer phalloidin oleate or the CDC42 inhibitor CASIN resulted in stunted filopodia outgrowth (Supplemental Figure 8A), reduced release of the large MP population (Supplemental Figure 8B), and decreased TF-specific activity on MPs to 46.5% ± 3.4% and 38.0% ± 1.4% of control, respectively.

Since lipid rafts regulate localization and function of TF and integrin β1 as well as PSGL1 (42–44), we asked whether rafts are required for receptor trafficking and incorporation into highly procoagulant MPs. In order to avoid effects of chronic depletion of cholesterol on TF induction (45, 46), we rapidly perturbed lipid raft dynamics by chelating cholesterol with a low concentration of filipin. Filipin had no significant effects on cellular TF activity, consistent with previous reports (47), but potently blocked ATP-induced release of TF activity on MPs (Figure 4A). PSGL1, TF, and integrin β1 were no longer incorporated into MPs in the presence of filipin (Figure 4B), but MP marker proteins γ-actin and PDI, which are targets for TRX, were still released and TRX and γ-actin were recovered in the cell supernatant (Figure 4, B and C).

FACS analysis confirmed the unaltered release of the large PS^+ MP population (95% ± 3% of control) in the presence of filipin, which also had no effect on functional PS-dependent MP prothrombinase activity (78% ± 36% of control). However, filipin markedly reduced TF expression on these MPs (20% ± 2% of control) (Figure 4D). Filipin did not interfere with ATP-induced formation of filopodia, but prevented the appearance of TF on filopodia (Figure 4E). Taken together, these data demonstrate raft-dependent trafficking of membrane receptors onto filopodia in the course of MP generation.

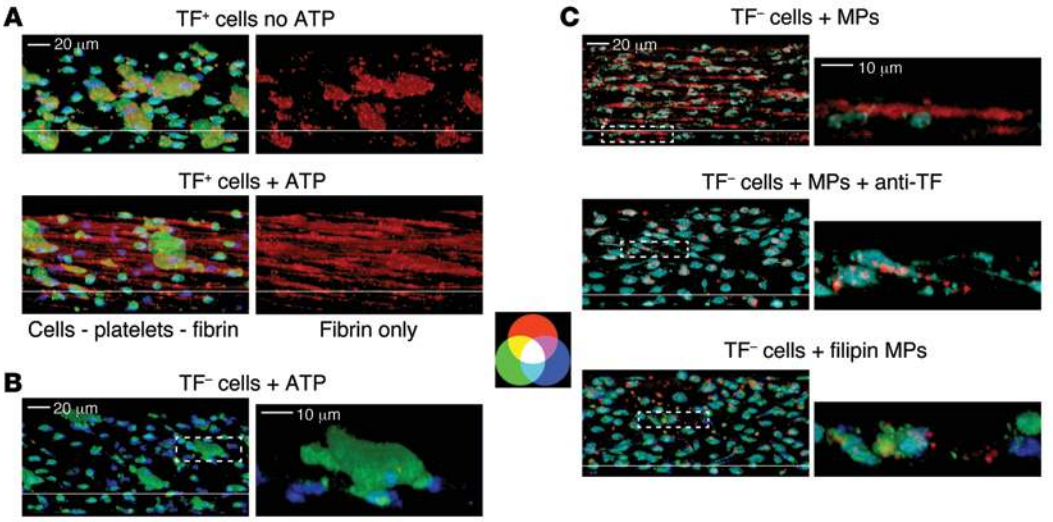

Figure 5. Macrophage-derived MPs are prothrombotic in flowing blood. Three-dimensional reconstruction of platelet aggregates and fibrin on surface-adherent macrophages was generated from confocal z-sections serially collected before and after blood perfusion. Images of green and red autofluorescent cells before flow were combined and converted to blue for superposition to corresponding images after flow. (**A**) Top left: LPS-primed macrophages exposed to recalcified flowing blood containing mepacrine (green) to visualize platelets and Alexa 546–labeled anti-fibrin antibody (red); merging of green, red, and blue yields the colors shown schematically at the center of the figure. Note that cells vary from blue to aqua owing to variable mepacrine incorporation from blood. Top right: Only the red component (fibrin) of the image on the left is shown. Bottom panels: Same as top, except that macrophages were stimulated with ATP (5 mM) before blood perfusion. (**B**) Mouse blood, treated as in **A**, was perfused over ATP-stimulated TF-deficient macrophages from *Tf*$^{fl/fl}$ *Lysm-Cre* mice. (**C**) Top panels: MPs from ATP-stimulated TFKI macrophages (expressing human TF) were added to blood before perfusion over TF-deficient, unstimulated macrophages. Note the appearance of fibrin strands. Middle panels: Species-specific anti–human TF antibody 5G9 was added with MPs to the blood before perfusion. No fibrin strands formed. Bottom panels: MPs from filipin-treated TFKI macrophages were perfused in blood over TF-deficient, unstimulated cells. In **B** and **C**, images on the right show a magnification of the area delimited by the white rectangle in the images on the left.

P2RX7-induced TF$^+$ *MPs promote fibrin strand formation in whole blood under flow*. We verified the procoagulant function of these macrophage-derived MPs in a more physiologically relevant whole blood environment. On the surface of LPS-primed WT macrophages exposed to recalcified flowing blood, limited amounts of fibrin formed that was associated primarily with platelet aggregates (Figure 5A, top panels). Following ATP stimulation of macrophages, fibrin associated with platelet aggregates was still present, but in addition long fibrin strands formed that extended in the direction of flow (Figure 5A, bottom panels). ATP simulation of LPS-primed but TF$^-$ macrophages induced negligible fibrin formation, although platelet clusters were still recruited around some cells (Figure 5B).

Adding isolated MPs derived from ATP-stimulated cells to blood before perfusion resulted in fibrin strand formation on the surface of TF-deficient, unstimulated macrophages (Figure 5C, top), in striking resemblance to the strands formed on ATP-stimulated WT cells except that there were no platelet aggregates with associated fibrin (compare with Figure 5A, bottom panels). Since the added MPs were generated from humanized TFKI mice, and species-selective antibodies against human TF blocked fibrin formation (Figure 5C, middle), these results showed that human TF on MPs and not blood-borne mouse TF activated by added MPs triggered prothrombotic activity. In addition, PS-expressing procoagulant MPs generated in the presence of filipin with severely reduced levels of raft-associated receptors, including TF, failed to form fibrin strands comparable to those seen with TF$^+$ MPs (Figure 5C, bottom). The similar pattern of fibrin deposition in flow-oriented strands that formed on ATP-stimulated WT macrophages or on TF$^-$ macrophages when blood contained procoagulant MPs suggests that de novo MP release from cells is a crucial factor for coagulation propagation in flowing blood.

Activation of the inflammasome is required for extracellular thiol-dependent MP release. TRX dissociation from TRX interacting protein (TXNIP) activates the inflammasome (48). Since TXNIP, unlike TRX, remained cell associated in P2RX7-stimulated cells (Supplemental Figure 9A), we next asked how inflammasome activation is coupled to extracellular thiol pathways and MP release. ROS of different sources can promote the dissociation of TRX and TXNIP, subsequent assembly of the NLRP3 inflammasome, and caspase-1 activation (49). Strikingly, we found that treating macrophages with niflumic acid (NFA), a selective inhibitor of endosomal ROS production (50), abrogated P2RX7-induced caspase-1 activation and TRX release (Figure 6A). Consistently, extracellular thiol appearance (Figure 6B), filopodia formation (Supplemental Figure 9B), and the downstream release of thromboinflammatory MPs (Supplemental Figure 9C) were blocked by NFA treatment. Since NFA also inhibits COX2, we excluded contributions of COX2 with the COX2 inhibitor rofecoxib and confirmed with another endosomal ROS inhibitor, 4,4′-diisothiocyano-2,2′-stilbenedisulfonic acid (DIDS) (51), the specificity of the NFA effects on TRX release, caspase-1 activation, and secretion of IL-1β (Supplemental Figure 9, B–D). NFA did not block total cellular ROS production (Supplemental Figure 9E), and cell surface receptors were consequently still released (Supplemental Figure 9F), pointing to a specific role of endosomal ROS for P2RX7-induced inflammasome activation and thromboinflammatory MP release.

We further evaluated the roles of inflammasome activation in MP release with the pharmacological inhibitors parthenolide

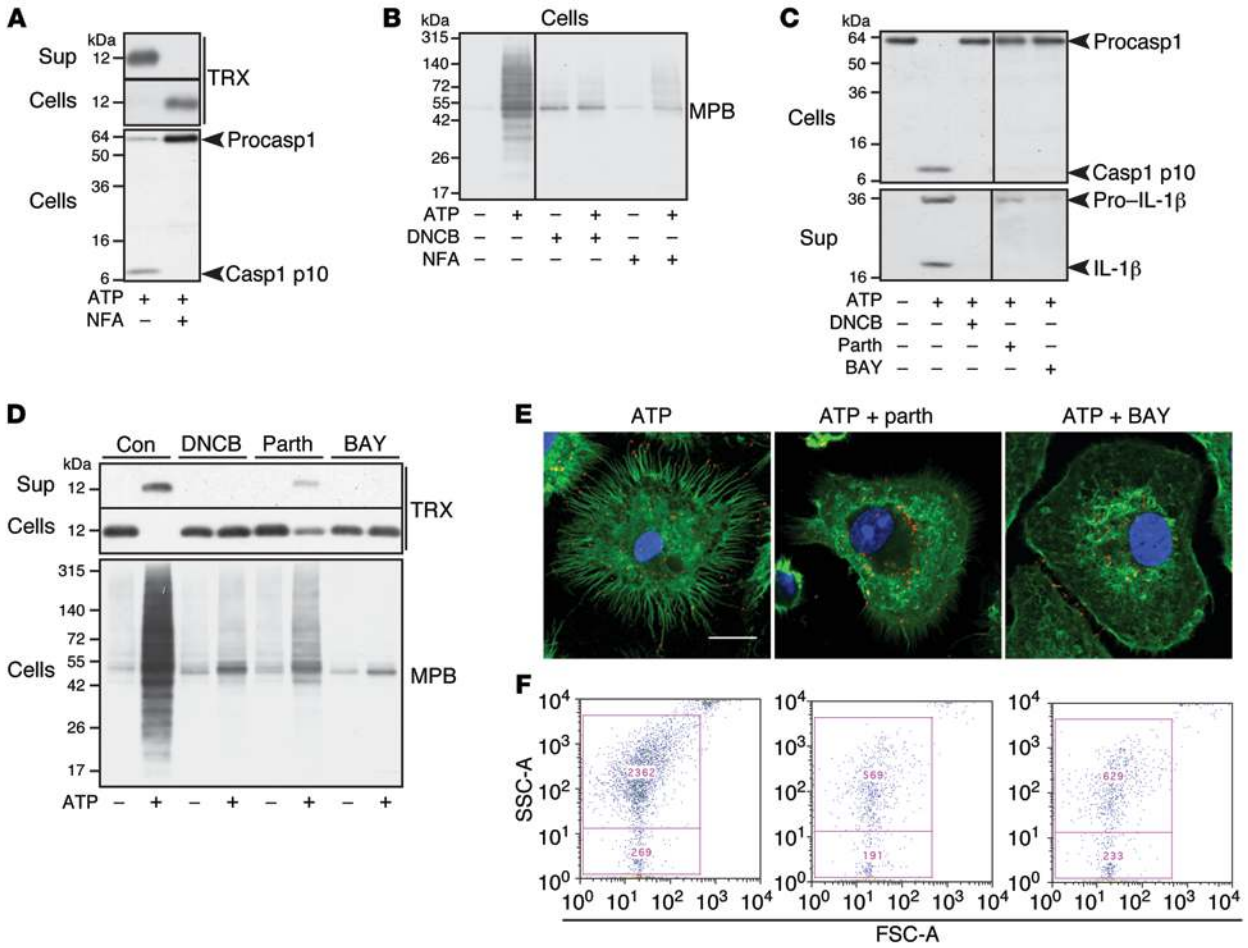

Figure 6. P2RX7-induced endosomal ROS are required for inflammasome activation and release of highly procoagulant MPs. (**A**) Effects of the endosomal ROS inhibitor niflumic acid (NFA) on caspase-1 activation and TRX release in ATP-stimulated cells and supernatants, as determined by Western blotting. (**B**) Streptavidin detection of MPB-labeled cell surface proteins on control, DNCB-pretreated, and NFA-pretreated cells with and without ATP stimulation. (**C** and **D**) Effects of DNCB and the inhibitors of inflammasome activity parthenolide (parth) and BAY 11-7082 (BAY) on ATP-induced activation of caspase-1 and IL-1β (**C**), and on release of TRX detected by Western blotting and the exposure of solvent-accessible free thiols on the cell surface detected by streptavidin blot (**D**). (**E**) Effects of inflammasome inhibitors on ATP-induced filopodia formation and TF translocation. Cell surface TF was stained with anti–TF–Alexa 647 conjugate (red) before stimulation. Fixed cells were counterstained for F-actin with phalloidin–Alexa 488 (green) and nuclei with Hoechst stain (blue); scale bar: 10 μm. (**F**) FACS analysis of MPs released from ATP-stimulated TFKI macrophages with or without inflammasome inhibitor pretreatment. Event counts are displayed in the gates of large and small MPs.

and BAY 11-7082 (52). As expected, both blocked ATP stimulation–induced caspase-1 activation and the subsequent processing and release of IL-1β (Figure 6C). Importantly, inhibitors of inflammasome activation also markedly attenuated the release of TRX and extracellular thiol appearance (Figure 6D), the formation of filopodia (Figure 6E), the generation of the typical large procoagulant MPs (Figure 6F) with TRX-target marker proteins (Supplemental Figure 9G), and release of MP TF activity (58.5% ± 7.7% in parthenolide-treated and 32.0% ± 1.7% in BAY 11-7082–treated cells compared with uninhibited control; $n = 3$, $P < 0.05$ and $P < 0.01$). These data demonstrate a novel role for inflammasome activation in promoting extracellular thiol modifications and coupling of thromboinflammatory responses of macrophages.

A caspase-1/calpain cysteine protease cascade releases TF from cytoskeletal anchoring during thiol-dependent MP release. We investigated additional contributions of inflammasome activation to the generation of highly procoagulant MPs. The cortical localization of surface TF in DNCB-treated cells suggested that a retention signal impaired trafficking of TF onto filopodia. TF is associated with cytoskeletal structures (53), and the cytoplasmic domain of TF interacts with filamin A (54) that anchors membrane proteins to the actin cytoskeleton (55). Proteolytic cleavage of filamin A by calpain (56) separates the 190-kDa actin-interacting domain from a 90-kDa carboxyl-terminal fragment involved in TF binding (54). We hypothesized that TF is retained by cytoskeletal anchoring and requires calpain-mediated filamin degradation for incorporation into MPs.

The endogenous inhibitor of calpain, calpastatin (56, 57), is degraded by cysteine proteases calpain and caspase-1 (58). ATP stimulation indeed induced calpastatin and filamin A degradation in WT macrophages, but not in *P2rx7*$^{-/-}$ macrophages (data not shown) or in the presence of DNCB (Figure 7A). As expected, the calpain inhibitor ALLN blocked cleavage of filamin A and calpastatin (Figure 7A). Calpain inhibition with ALLN had no effect

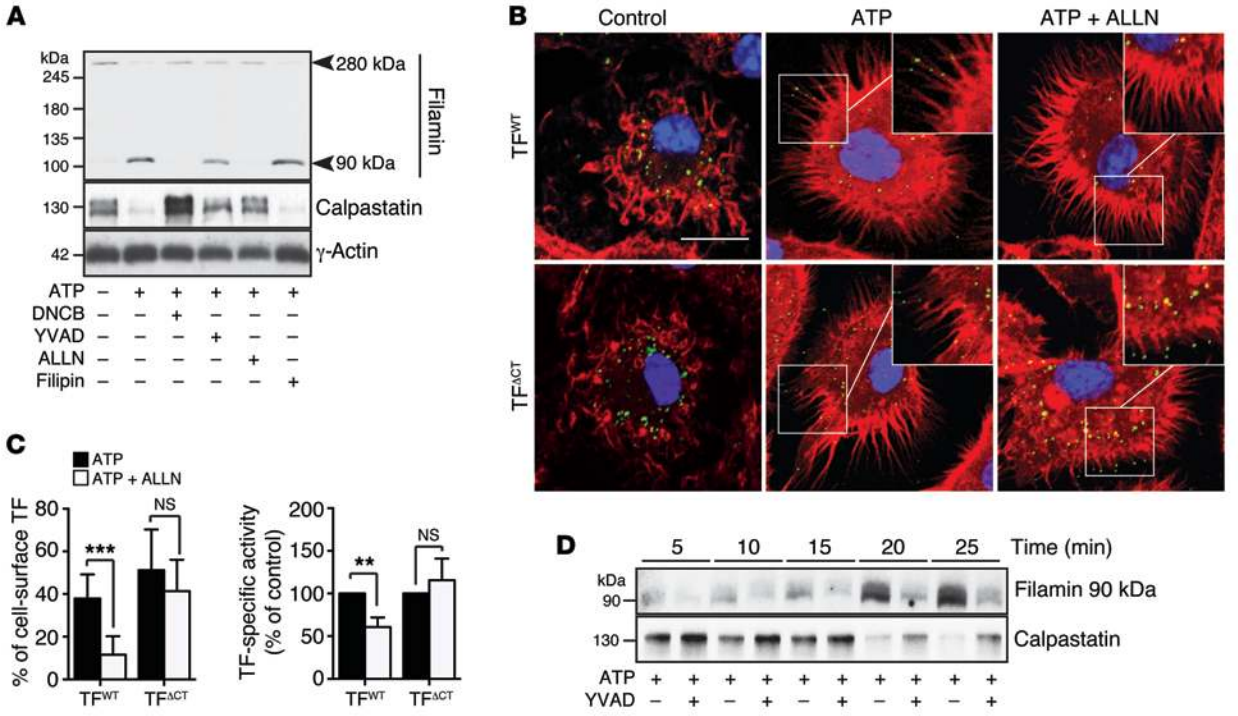

Figure 7. P2RX7 signaling–activated cysteine proteases regulate TF trafficking. (**A**) Effects of inhibitors of TRXR (DNCB), caspase-1 (YVAD), calpain (ALLN), or lipid rafts (filipin) on ATP-induced degradation of filamin and calpastatin detected by Western blotting. Detection of cellular γ-actin served as loading control. (**B**) Effects of ALLN on TF localization in control and following ATP stimulation of WT (TF^{WT}) or TF cytoplasmic domain–deleted ($TF^{\Delta CT}$) macrophages. Cell surface TF was labeled with immunopurified rabbit anti–mouse TF antibody before the MP release reaction. Fixed cells were counterstained with Alexa 488–conjugated anti-rabbit IgG (green), phalloidin–Alexa 546 (red), and Hoechst (blue); scale bar: 10 μm. (**C**) Quantification of TF localized on filopodia; mean ± SD, $n \geq 12$, $^{***}P < 0.001$, *t* test. TF-specific activity on MPs from ATP-stimulated TF^{WT} and $TF^{\Delta CT}$ macrophages in the absence or presence of ALLN was determined based on normalization of MP-released TF quantified by Western blotting; mean ± SD, $n = 3$, $^{**}P < 0.01$, *t* test. (**D**) Western blot analysis of a time course of ATP-induced filamin and calpastatin degradation in control and in caspase-1 inhibitor–treated cells.

on MP release (Supplemental Figure 10, A and B) or the appearance of extracellular thiols (Supplemental Figure 10C), but ALLN treatment prevented the ATP-induced translocation of TF onto filopodia (Figure 7B). ALLN caused significantly reduced TF-specific activity on MPs (Figure 7C), particularly the activity on MPs that were released for prolonged times (Supplemental Figure 10D), and decreased the number of MPs incorporating both TF and PS (Supplemental Figure 9E).

In sharp contrast, deletion of the TF cytoplasmic domain linking TF to filamin A (54) prevented effects of ALLN and restored efficient translocation of TF onto filopodia, and increased TF-specific activity relative to ALLN inhibited WT macrophages (Figure 7, B and C). Blocking caspase-1 activity by incubation with the specific inhibitor YVAD considerably delayed calpain activation relative to control cells (Figure 7, A and D), resulting in reduced filamin A cleavage (33% ± 0.1%) and increased calpastatin levels (2.7 ± 0.3–fold) after 30 minutes of ATP stimulation, positioning TRXR upstream of a caspase-1–initiated cysteine protease cascade. Taken together, these results show that filamin degradation eliminates a bond between TF and the cytoskeleton, facilitating TF transport onto filopodia for incorporation into PS-rich MPs. Additional experiments with ATP-stimulated, smooth muscle cells expressing the P2RX7 confirmed more generally the crucial role of calpain-mediated filamin degradation for TF release on procoagulant MPs (Supplemental Figure 10, F and G).

Caspase-1 is required for extracellular actin-dependent MP generation. The following experiments uncovered additional calpain-independent roles of caspase-1 in the thromboinflammatory release pathway of macrophages. As expected, incubation with the caspase-1 inhibitor YVAD completely prevented P2RX7-induced processing of IL-1β but had no effect on inflammasome activation, as evidenced by generation of the caspase-1 p10 proteolytic fragment (Figure 8A). Furthermore, incubating cells with YVAD did not affect ATP-induced release of TRX into the extracellular space (Figure 8A) and reductive changes on the cell surface (Figure 8B). As predicted from the position of caspase-1 upstream of calpain, caspase-1 blockade caused retention of TF in the cell body; unexpectedly, it also changed the appearance of filopodia, increasing their length (Figure 8C), and led to an overall flatter shape of ATP-stimulated macrophages (Supplemental Videos 5 and 6).

Surprisingly, caspase-1 inhibition prevented the appearance of thiol-labeled proteins in the MP fraction (Figure 8B), including γ-actin and PDI (Supplemental Figure 11A), as well as the generation of the typical large procoagulant MP population (Figure 8D). Accordingly, TF-specific MP activity was reduced to 39.5% ± 12.1% of control ($n = 3$, $P < 0.01$, *t* test), and the prolonged release of cell surface receptors on MPs collected after 15 minutes of stimulation was reduced in caspase-1–blocked cells (Supplemental Figure 11, A–C). Although no difference in thiol labeling was observed between control and caspase-1–blocked

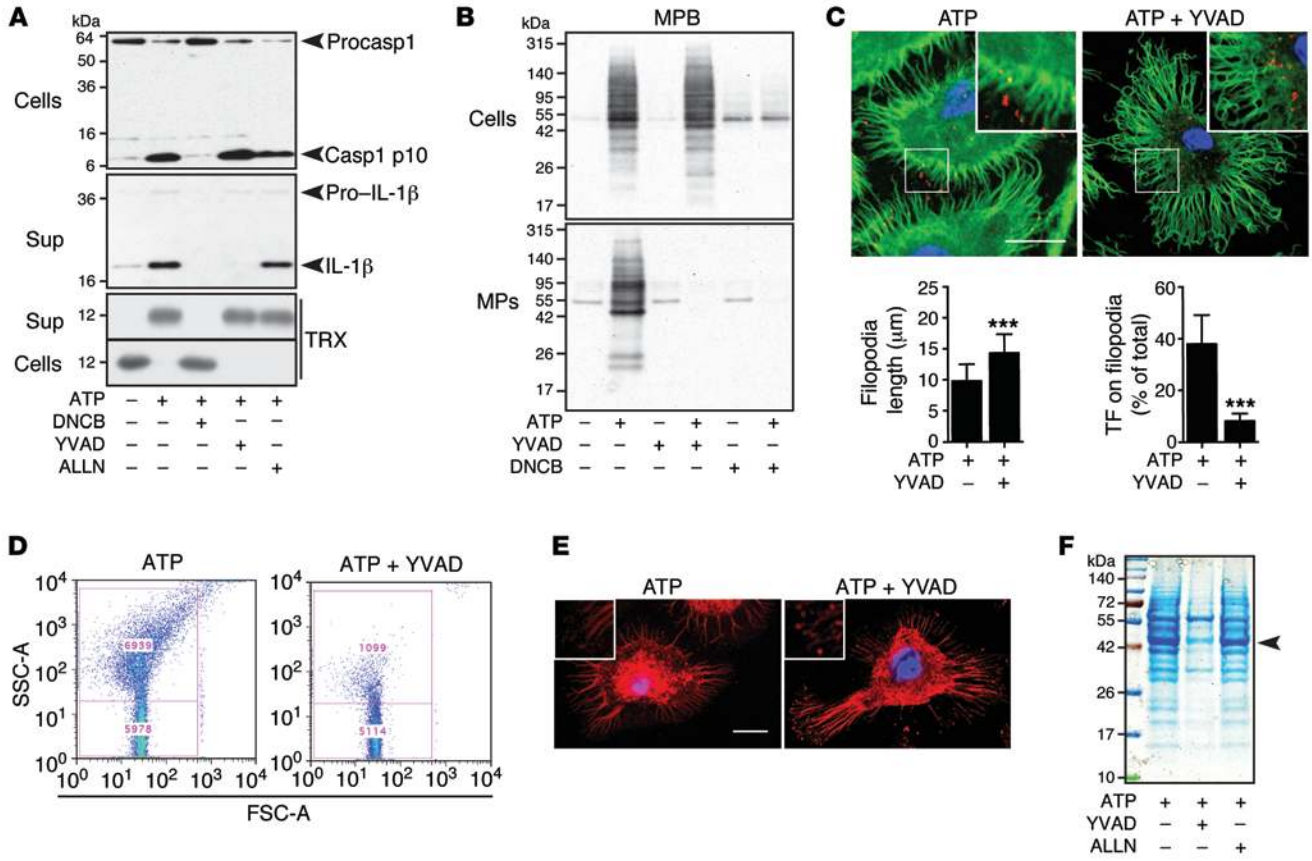

Figure 8. Caspase-1 activity is required for thromboinflammatory MP generation. (**A**) Effects of inhibitors of TRXR (DNCB), caspase-1 (YVAD), and calpain (ALLN) on ATP-induced activation of caspase-1 and IL-1β, and secretion of TRX detected by Western blotting. (**B**) Streptavidin blots of MPB-labeled free thiol groups on cells and MPs generated in the presence or absence of YVAD or DNCB. (**C**) Effects of YVAD on ATP-induced filopodia formation and TF translocation. TF was stained with anti–TF–Alexa 647 conjugate (red) before stimulation. Fixed and permeabilized cells were counterstained for F-actin (green) and nuclei (blue); scale bar: 10 μm. Length of filopodia and appearance of TF on filopodia were assessed; mean ± SD, $n = 4$, $^{***}P < 0.001$, t test. (**D**) ATP-induced MPs from control and YVAD-pretreated cells detected by FACS. (**E**) Confocal imaging of continuously MPB-labeled cells stimulated with ATP with or without YVAD. MPB was detected with Texas Red–labeled streptavidin (red) and nuclei with DAPI (blue) after fixation; scale bar: 10 μm. (**F**) Coomassie blue staining of proteins in the MP-depleted supernatants of ATP-stimulated cells with or without YVAD or ALLN treatment. TFKI macrophages were used for FACS analysis and confocal imaging.

cells when MPB was added during ATP stimulation, labeling free thiols at the end of the reaction showed reduced solvent-accessible free thiols in caspase-1–blocked cells (Supplemental Figure 11D), indicating that surface thiol exposure was less stable because of secondary cell surface events.

Confocal imaging localized cell surface thiols to the cell body and filopodia (Figure 8E), but surface thiol labeling was not detectable in TRXR-inhibited cells (Supplemental Figure 11E). Caspase-1 blockade had no major effect on thiol exposure on the cell surface, but led to an accumulation of thiol-labeled vesicular structures at the tips of filopodia (Figure 8E), indicating that the final release of highly procoagulant MPs from filopodia required proteolytic activity of caspase-1. Experiments in caspase-1–deficient cells confirmed the crucial role in the generation of thromboinflammatory MPs (Supplemental Figure 12, A–F). Extracellular vesicles containing predominantly unactivated components of the inflammasome and pro–IL-1β are slowly released from cultured monocytes primed with LPS alone (29). In contrast, additional triggering of P2RX7 by the second-hit signal ATP led to rapid cellular activation of the inflammasome. Whereas the inflammasome component NLRP3 was cell associated and in the supernatant, the released MPs contained activated caspase-1, but not processed IL-1β, which was predominantly detected in the MP-depleted supernatant (Supplemental Figure 13A). In DNCB-blocked cells, no uncleaved caspase-1 was seen on the released MPs (Supplemental Figure 13B). These findings are consistent with specific physical association of active caspase-1 with budding MPs during thromboinflammatory MP release.

Consistent with the concept that the release of soluble proteins is mechanistically linked to the generation of thromboinflammatory MPs, inhibition of caspase-1, but not of calpain, markedly reduced the appearance of γ-actin and other proteins in the extracellular space (Figure 8F). The small amount of actin detected in caspase-1–blocked supernatants had slower mobility as compared with actin released from ATP-stimulated cells with a functional caspase-1, indicating caspase-1–dependent cleavage. Importantly, staining of nonpermeabilized cells with cell-impermeable, fluorophore-labeled phalloidin showed that ATP stimulation induced a TRXR-dependent cell surface appearance of actin that particularly decorated filopodia. In contrast, and despite actin remodeling doc-

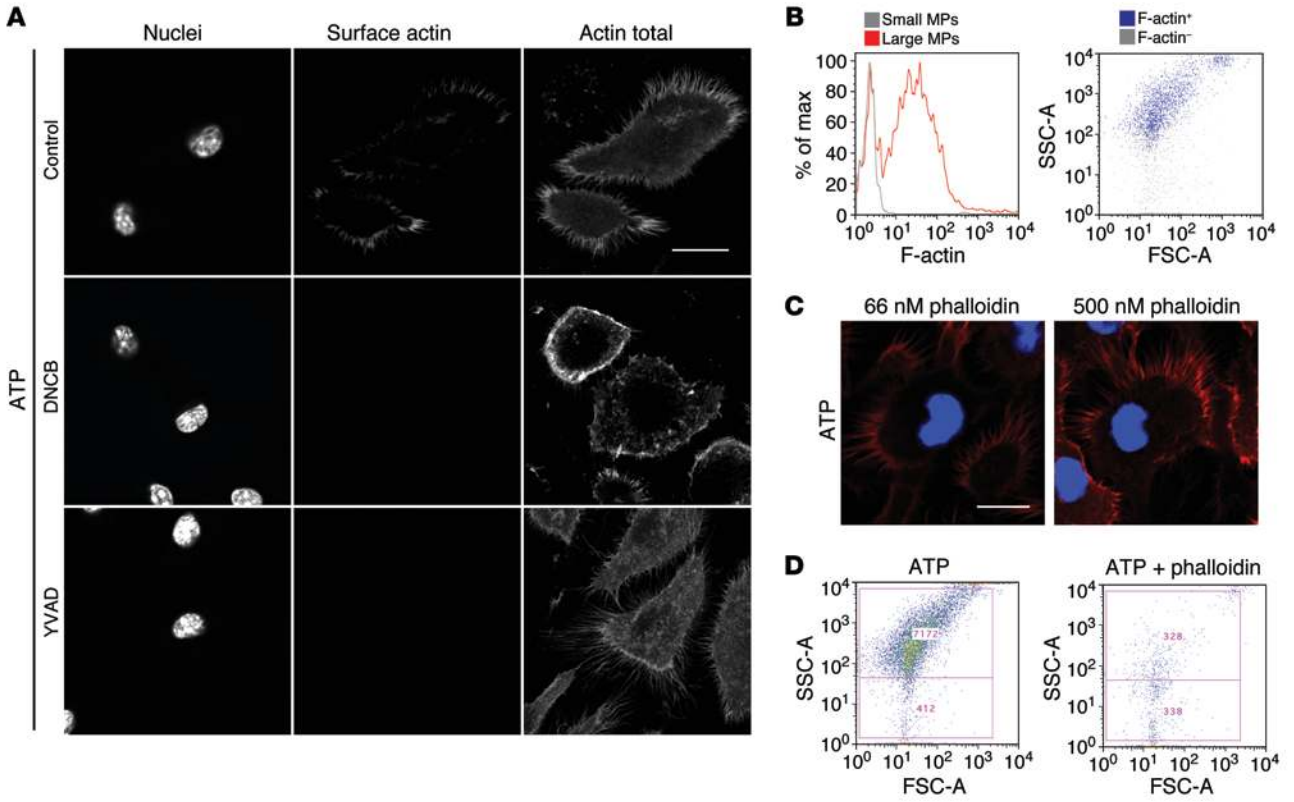

Figure 9. F-actin is exposed on the cell surface during MP generation. (**A**) Surface F-actin was detected by phalloidin staining of nonpermeabilized ATP-stimulated cells (middle panel) using phalloidin–Alexa 633 conjugates, and counterstained for total F-actin (right panel) with phalloidin–Alexa 488 conjugates and nuclei with Hoechst after fixation. Cells were pretreated with DNCB or YVAD, as indicated; scale bar: 20 μm. (**B**) Detection of F-actin on ATP-induced MP populations by FACS using phalloidin–Alexa 633 conjugates. (**C**) Confocal images of ATP-stimulated cells in the presence of phalloidin–Alexa 546 concentrations used for cell staining (66 nM) or MP release blocking experiments (500 nM) demonstrate that higher concentration of phalloidin did not inhibit filopodia formation. (**D**) Abundance of ATP-induced MPs detected by FACS from control cells and from cells stimulated in the presence of cell-impermeable phalloidin to block extracellular actin. TFKI macrophages were used for FACS analysis and confocal imaging.

umented by intracellular actin staining in filopodia, surface actin was not detectable on caspase-1–blocked cells (Figure 9A).

These data suggested that extracellular actin might play a functional role in the release of highly procoagulant MPs. In support of this conclusion, F-actin was detected by phalloidin staining on the MP surface, specifically of large MPs generated dependent on TRXR and inflammasome activation (Figure 9B). Although the development of filopodia appeared to be unperturbed (Figure 9C), addition of high concentrations of cell-impermeable phalloidin during the stimulation with ATP inhibited the release of large MPs (Figure 9D), implicating cell surface–exposed F-actin directly in MP biogenesis. These data demonstrate an entirely unexpected role for caspase-1–mediated extracellular actin exposure in the final severing of prothrombotic MPs from filopodia and thus position this protease as a central mediator for proinflammatory and procoagulant macrophage responses in thrombosis and cardiovascular diseases.

Discussion

Here, we delineate key events required for prothrombotic MP generation following injury signal–induced activation of macrophage P2X7 receptors (Figure 10). In this pathway, TRXR is crucial for several steps that ultimately lead to the incorporation of cell surface receptors into MPs with a distinct composition of proteins that are targets of TRX and a high surface density of procoagulant PS. Together with released soluble proteins, these proteomes are reflective of mechanistic details of the MP release reaction and may provide diagnostic fingerprints for detecting thromboinflammatory activation of macrophages in complex biological samples.

Following P2RX7 activation, functional TRXR promotes the cellular release of its substrate TRX in a reduced form and thereby prevents intracellular TRX regulatory functions and causes extracellular reductive changes required for generation of a distinct MP population. Actin residue Cys374 is reversibly modified by TRX and controls actin dynamics (59). Furthermore, the TRX substrate PDI promotes actin polymerization at membrane protrusions (60), providing an explanation for TRXR-dependent filopodia formation and the incorporation of these marker proteins into MPs generated following actin remodeling.

Dissociation of TRX from TXNIP furthermore leads to inflammasome activation. Although ROS derived from damaged mitochondria (49) have been shown to mediate spatially controlled activation of the inflammasome, our experiments with chloride channel inhibitors that block superoxide efflux from the endosome indicate that endosomal ROS are specifically required for P2RX7-mediated rapid activation of the inflammasome. This

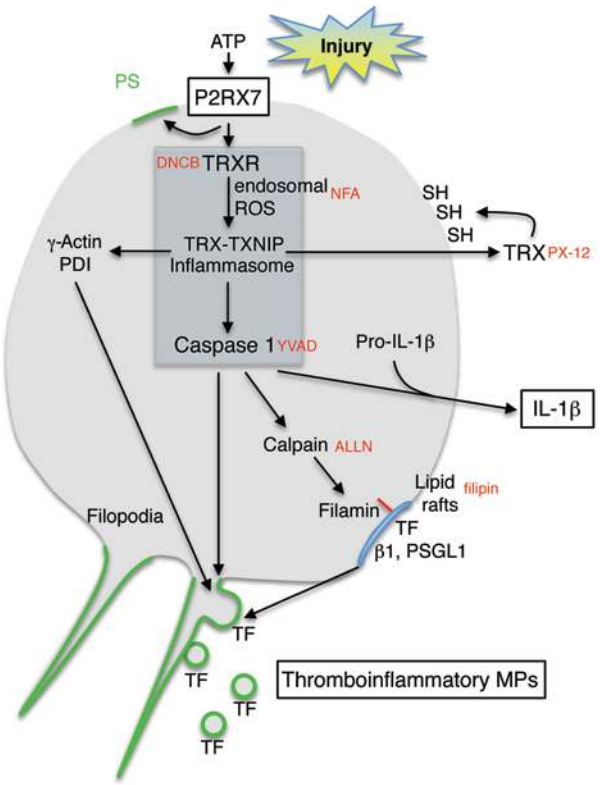

Figure 10. Schematic illustration of the proposed thromboinflammatory MP release pathway in macrophages. Macrophage priming by IFN-γ and TLR ligands induces transcriptional upregulation of TF and proinflammatory interleukins. Activation of the macrophage P2RX7 by ATP triggers TRXR-dependent release of TRX, leading to reductive changes of the extracellular proteome, as indicated by the extracellular free thiol (SH) groups. The intracellular depletion of TRX abolishes regulatory functions of TRX and causes actin remodeling and filopodia formation as well as TXNIP-mediated inflammasome assembly and caspase-1 activation. Active caspase-1 mediates maturation and release of the proinflammatory cytokine IL-1β and facilitates activation of calpain, which in turn reverses TF retention by filamin (indicated as a red rod on the cytoplasmic side of TF) and thereby allows raft-dependent trafficking of TF onto filopodia. Membrane receptors TF, integrin β1, and PSGL1 assemble with marker proteins of highly procoagulant MPs, γ-actin, and PDI when released from PS-rich filopodia, facilitated by caspase-1 and resulting in highly procoagulant thromboinflammatory MPs. Key pharmacological inhibitors used here are placed next to their targets to indicate where the thromboinflammatory pathway is inhibited.

process is likely induced by P2RX7 engagement by ATP causing endosomal receptor uptake (61). Moreover, P2RX7-dependent inflammasome activation promotes a caspase-1/calpain cysteine cascade leading to filamin degradation, the severing of cytoskeletal retention of TF, and raft-dependent receptor incorporation into highly procoagulant MPs.

Unexpectedly, caspase-1 has a calpain-independent pivotal role in the final release of procoagulant MPs. In the presence of functional caspase-1, inflammasome activation causes the extracellular appearance of actin that decorates the surface of extending filopodia, suggesting considerable membrane instability allowing for actin translocation. Actin-associated proteins, including annexins 1 and 5, are also released dependent on caspase-1 activity and may stabilize the P2RX7-induced but TRXR- and caspase-1–independent flip of PS to the outer membrane. The extracellular appearance of these proteins in conjunction with the membrane curvature of filopodia may favor the concentration of negatively charged phospholipids on released MPs (62, 63). Thus, the effector protease of the inflammasome pathway is at the center of the coupling of inflammation and thrombosis.

We confirmed in flowing blood that MPs generated by this pathway are highly thrombogenic and promote fibrin strand formation extending even from otherwise unperturbed and quiescent cell surfaces. While TF was required for these prothrombotic effects, interaction of MP TF with its signaling receptor on host cells can increase TF-bearing particle uptake and moreover promotes intracellular signaling (64, 65). Consistently, an expanding literature documents active uptake of MPs and exosomes by vascular wall cells promoting inflammation (29, 66) and proangiogenic trans-signaling (65, 67). The current identification of MP proteome composition governed by specific agonist pathways represents a first step toward studies that define biological effects beyond thrombosis by distinct MP populations carrying TF.

Although not addressed experimentally here, extracellular thiol-disulfide exchange in the context of surface exposure of procoagulant PS may contribute to procoagulant activation of what is referred to as cryptic cell surface TF. Given the redox potential (68) and biochemical evidence for TRX-mediated reduction (69) of the TF allosteric disulfide bond (70, 71), extracellular TRX may initiate thiol-disulfide exchange leading to reshuffling of this bond in cell surface–localized but coagulation-inactive TF. The demonstrated progressive oxidation of extracellular TRX in turn may cause subsequent PDI chaperone activity–supported (72) TF reoxidation in a PS-localized conformation, in analogy to PDI-dependent TF activation in the context of complement activation (13). Extracellular TRX may influence additional redox targets (73) and thereby more generally promote coagulation reactions contributing to hemostasis and thrombosis.

The TRX/TRXR system plays important regulatory roles in biological responses to oxidative stress and redox signaling in cardiovascular diseases (74, 75), and serum levels of TRX are elevated significantly in patients with coronary syndromes with as-yet unclear pathogenetic implications (76). We provide novel mechanistic insight into the significance of extracellular TRX as a potential biomarker in cardiovascular diseases by demonstrating that the release of TRX indicates not only inflammatory IL-1β production, but also increased thrombogenicity of innate immune cells. Efforts are under way to utilize IL-1β levels for risk stratification and to target IL-1β for cardiovascular prevention (6, 77). However, the pathway delineated here provides evidence that additional pharmacological targets may provide benefits by simultaneously attenuating inflammation and innate immune cell–induced thrombosis.

Although the P2RX7 thromboinflammatory pathway of TF activation and release is discussed here primarily in the context of atherosclerosis, evidence suggests its implication in various diseases. For instance, clinical data indicate a critical role of P2RX7 in sepsis (78), which is particularly intriguing since bacterial LPS potently promotes TF upregulation. Indeed, increased TF^+ MP levels correlate with hypercoagulability in endotoxemic mice (79), and extracellular TRX levels are significantly elevated in plasma of sepsis patients (80). Similarly, P2RX7 signaling is implicated in rheumatoid arthritis (81), and high levels of extracellular TRX (82, 83) as well as of TF^+ MPs (84) are detected in the synovial fluids of patients. Notably, the TRXR inhibitor auranofin is efficacious in the treatment of rheumatoid arthritis. In light of the common role of caspase-1 in proinflammatory IL-1β activation and procoagulant MP release, it is tempting to speculate that the thromboinflammatory response pathway identified here is of broad clinical significance.

Methods

Extended experimental procedures and methods are described in the Supplemental Methods.

MP release assay with primary bone marrow–derived macrophages. Bone marrow–derived macrophages from C57BL/6J, $Tf^{fl/fl}$ *Lysm-Cre* mice (85), human TF knock-in (TFKI) mice (34), or caspase-1–deficient mice (86) were generated as previously described (12). Briefly, bone marrow cells were cultivated in DMEM containing 20% L cell medium, 10% FCS, 1 mM L-glutamine, and penicillin and streptomycin. The medium was exchanged on day 6, and on day 7 macrophages were seeded at 1×10^6 per well in a 12-well plate and primed with 100 ng/ml IFN-γ (PeproTech) overnight. On the following day, macrophages were stimulated with 1 mg/ml LPS (*Salmonella abortus equi*; Enzo Life Sciences) for 4 hours. Cells were pretreated for 30 minutes with DNCB (30 mM; Sigma-Aldrich), parthenolide (10 mM; Cayman Chemical), BAY 11-7082 (12 mM; Cayman Chemical), DPI (100 mM; Sigma-Aldrich), or NFA (30 mM; Sigma-Aldrich) or immediately before ATP stimulation with PAO (10 mM; Sigma-Aldrich), filipin (5 mg/ml; Sigma-Aldrich), ALLN (1 mM; EMB Millipore), or Ac-YVAD-CMK (10 mM; Enzo Life Sciences). Cells were rinsed once in BSS buffer (0.13 M Na-gluconate, 0.02 M HEPES, 5 mM glucose, 5 mM glycine, 5 mM KCl, 1 mM $MgCl_2$, pH 7.5) and then exposed in the same buffer to 5 mM ATP (Roche Applied Science) for 30 minutes or as indicated. Upon removal of cell debris (1,000 *g*, 10 minutes), MPs were isolated by centrifugation at 16,000 *g* for 60 minutes for functional assays, and supernatants were precipitated with TCA for Western blotting, using established procedures (12) with reagents described in detail in the extended Supplemental Methods section.

Protein identification and flow cytometry. MPs were recovered from concentrated cell-free supernatant by centrifugation, and proteins separated by SDS-PAGE were isolated on the basis of the location of thiol-labeled bands on adjacent lanes for identification by nano-LC-MS/MS at The Scripps Research Institute Center for Mass Spectrometry. MPs were further analyzed on an LSR-II flow cytometer (BD Biosciences) calibrated with a defined platelet suspension of Megamix beads, as previously described (87). Cell-free MP suspensions were stained with anti–human TF 9C3–Alexa 647 conjugate (5 mg/ml) and lactadherin-FITC (0.5 mg/ml; Haematologic Technologies), and data were analyzed using FlowJo software (Tree Star).

Microscopy. MP procoagulant activity on cell surfaces was evaluated in flow chamber experiments with whole blood using confocal microscopy and quantitative image analysis, as previously described (12). Cells stained and mounted as described in detail in the Supplemental Methods were analyzed using a ×63 oil immersion objective on a Zeiss 710 LSM, and images were processed with Image Browser (Zeiss) and Imaris (Bitplane) image analysis software.

Statistics. Statistical analysis was performed using Prism 6 software (GraphPad Software). For statistics comparing 2 groups, the *t* test (2-sided) was used, and for statistical analysis of more then 2 groups, 1-way ANOVA with Bonferroni multiple comparison correction was used. For all tests at least 3 independent experiments were analyzed, and *P* values of less than $P < 0.05$ were considered significant.

Study approval. Animal procedures were approved by the IACUC of The Scripps Research Institute.

Acknowledgments

We greatly appreciate the excellent technical assistance by Cynthia Biazak, Pablito Tejada, and Jennifer Royce. This study was supported by NIH grants P01-HL031950 (to W. Ruf, Z.M. Ruggeri, and M.H. Ginsberg) and R01-HL077753 (to W. Ruf) and a fellowship of the Deutsche Forschungsgemeinschaft (RO 3795/2-1) and NovoNordisk (to A.S. Rothmeier).

Address correspondence to: Wolfram Ruf, Department of Immunology and Microbial Science, The Scripps Research Institute, 10550 North Torrey Pines Road, La Jolla, California 92037, USA. Phone: 858.784.2784; E-mail: ruf@scripps.edu.

1. Libby P, Lichtman AH, Hansson GK. Immune effector mechanisms implicated in atherosclerosis: from mice to humans. *Immunity*. 2013;38(6):1092–1104.
2. Dinarello CA. Interleukin-1 in the pathogenesis and treatment of inflammatory diseases. *Blood*. 2011;117(14):3720–3732.
3. Boyle JJ. Macrophage activation in atherosclerosis: pathogenesis and pharmacology of plaque rupture. *Curr Vasc Pharmacol*. 2005;3(1):63–68.
4. Toschi V, et al. Tissue factor modulates the thrombogenicity of human atherosclerotic plaques. *Circulation*. 1997;95(3):594–599.
5. Ruf W, Edgington TS. Structural biology of tissue factor, the initiator of thrombogenesis in vivo. *FASEB J*. 1994;8(6):385–390.
6. Qamar A, Rader DJ. Effect of interleukin 1β inhibition in cardiovascular disease. *Curr Opin Lipidol*. 2012;23(6):548–553.
7. Curtiss LK, Tobias PS. Emerging role of Toll-like receptors in atherosclerosis. *J Lipid Res*. 2009;50(suppl):S340–S345.
8. Duewell P, et al. NLRP3 inflammasomes are required for atherogenesis and activated by cholesterol crystals. *Nature*. 2010;464(7293):1357–1361.
9. Netea MG, et al. Differential requirement for the activation of the inflammasome for processing and release of IL-1beta in monocytes and macrophages. *Blood*. 2009;113(10):2324–2335.
10. Dubyak GR. P2X7 receptor regulation of non-classical secretion from immune effector cells. *Cell Microbiol*. 2012;14(11):1697–1706.
11. Owens AP, et al. Monocyte tissue factor-dependent activation of coagulation in hypercholesterolemic mice and monkeys is inhibited by simvastatin. *J Clin Invest*. 2012;122(2):558–568.
12. Furlan-Freguia C, Marchese P, Gruber A, Ruggeri ZM, Ruf W. P2X7 receptor signaling contributes to tissue factor-dependent thrombosis in mice. *J Clin Invest*. 2011;121(7):2932–2944.
13. Langer F, et al. Rapid activation of monocyte tissue factor by antithymocyte globulin is dependent on complement and protein disulfide isomerase. *Blood*. 2013;121(12):2324–2335.
14. Langer F, Ruf W. Synergies of phosphatidylserine and protein disulfide isomerase in tissue factor activation. *Thromb Haemost*. 2014;111(4):590–597.
15. Popescu NI, Lupu C, Lupu F. Extracellular protein

disulfide isomerase regulates coagulation on endothelial cells through modulation of phosphatidylserine exposure. *Blood*. 2010;116(6):993–1001.
16. Cho J, et al. Protein disulfide isomerase capture during thrombus formation in vivo depends on the presence of beta3 integrins. *Blood*. 2012;120(3):647–655.
17. Lahav J, et al. Enzymatically catalyzed disulfide exchange is required for platelet adhesion to collagen via integrin a2b1. *Blood*. 2003;102(6):2085–2092.
18. Ferrari D, et al. The P2X7 receptor: a key player in IL-1 processing and release. *J Immunol*. 2006;176(7):3877–3883.
19. Di Virgilio F. Liaisons dangereuses: P2X(7) the inflammasome. *Trends Pharmacol Sci*. 2007;28(9):465–472.
20. Lee R, Williams JC, Mackman N. P2X7 regulation of macrophage tissue factor activity microparticle generation. *J Thromb Haemost*. 2012;10(9):1965–1967.
21. Darbousset R, et al. P2X1 expressed on polymorphonuclear neutrophils platelets is required for thrombosis in mice. *Blood*. 2014;124(16):2575–2585.
22. Erhardt JA, Toomey JR, Douglas SA, Johns DG. P2X1 stimulation promotes thrombin receptor-mediated platelet aggregation. *J Thromb Haemost*. 2006;4(4):882–890.
23. Falzoni S, Donvito G, Di Virgilio F. Detecting adenosine triphosphate in the pericellular space. *Interface Focus*. 2013;3(3):20120101.
24. Piscopiello M, et al. P2X7 receptor is expressed in human vessels and might play a role in atherosclerosis. *Int J Cardiol*. 2013;168(3):2863–2866.
25. Falati S, et al. Accumulation of tissue factor into developing thrombi in vivo is dependent upon microparticle P-selectin glycoprotein ligand 1 and platelet P-selectin. *J Exp Med*. 2003;197(11):1585–1598.
26. Giesen PLA, et al. Blood-borne tissue factor: another view of thrombosis. *Proc Natl Acad Sci U S A*. 1999;96(5):2311–2315.
27. Rautou PE, et al. Microparticles, vascular function, and atherothrombosis. *Circ Res*. 2011;109(5):593–606.
28. Bernimoulin M, et al. Differential stimulation of monocytic cells results in distinct populations of microparticles. *J Thromb Haemost*. 2009;7(6):1019–1028.
29. Wang JG, et al. Monocytic microparticles activate endothelial cells in an IL-1β-dependent manner. *Blood*. 2011;118(8):2366–2374.
30. Arner ES, Bjornstedt M, Holmgren A. 1-Chloro-2,4-dinitrobenzene is an irreversible inhibitor of human thioredoxin reductase. Loss of thioredoxin disulfide reductase activity is accompanied by a large increase in NADPH oxidase activity. *J Biol Chem*. 1995;270(8):3479–3482.
31. Lassing I, et al. Molecular and structural basis for redox regulation of β-actin. *J Mol Biol*. 2007;370(2):331–348.
32. Wang X, et al. Redox regulation of actin by thioredoxin-1 is mediated by the interaction of the proteins via cysteine 62. *Antioxid Redox Signal*. 2010;13(5):565–573.
33. Taketo M, Matsui M, Rochelle JM, Yodoi J, Seldin MF. Mouse thioredoxin gene maps on chromosome 4, whereas its pseudogene maps on chromosome 1. *Genomics*. 1994;21(1):251–253.
34. Snyder LA, et al. Expression of human tissue factor under the control of the mouse tissue factor promoter mediates normal hemostasis in knock-in mice. *J Thromb Haemost*. 2008;6(2):306–314.
35. Shi J, Shi Y, Waehrens LN, Rasmussen JT, Heegaard CW, Gilbert GE. Lactadherin detects early phosphatidylserine exposure on immortalized leukemia cells undergoing programmed cell death. *Cytometry A*. 2006;69(12):1193–1201.
36. Gromer S, Arscott LD, Williams CH, Williams CH Jr, Schirmer RH, Becker K. Human placenta thioredoxin reductase. Isolation of the selenoenzyme, steady state kinetics, and inhibition by therapeutic gold compounds. *J Biol Chem*. 1998;273(32):20096–20101.
37. Kirkpatrick DL, et al. Mechanisms of inhibition of the thioredoxin growth factor system by antitumor 2-imidazolyl disulfides. *Biochem Pharmacol*. 1998;55(7):987–994.
38. Diakonova M, Gerke V, Ernst J, Liautard JP, van der Vusse G, Griffiths G. Localization of five annexins in J774 macrophages on isolated phagosomes. *J Cell Sci*. 1997;110(pt 10):1199–1213.
39. Patel DM, Ahmad SF, Weiss DG, Gerke V, Kuznetsov SA. Annexin A1 is a new functional linker between actin filaments phagosomes during phagocytosis. *J Cell Sci*. 2011;124(pt 4):578–588.
40. Ruf W, Edgington TS. An anti-tissue factor monoclonal antibody which inhibits TF:VIIa complex is a potent anticoagulant in plasma. *Thromb Haemost*. 1991;66(5):529–533.
41. Mandal SK, Pendurthi UR, Rao LV. Tissue factor trafficking in fibroblasts: involvement of protease-activated receptor-mediated cell signaling. *Blood*. 2007;110(1):161–170.
42. Mandal SK, Pendurthi UR, Rao LV. Cellular localization and trafficking of tissue factor. *Blood*. 2006;107(12):4746–4753.
43. Leitinger B, Hogg N. The involvement of lipid rafts in the regulation of integrin function. *J Cell Sci*. 2002;115(pt 5):963–972.
44. Stadtmann A, et al. The PSGL-1-L-selectin signaling complex regulates neutrophil adhesion under flow. *J Exp Med*. 2013;210(11):2171–2180.
45. Triantafilou M, Miyake K, Golenbock DT, Triantafilou K. Mediators of innate immune recognition of bacteria concentrate in lipid rafts and facilitate lipopolysaccharide-induced cell activation. *J Cell Sci*. 2002;115(pt 12):2603–2611.
46. Banfi C, et al. Tissue factor induction by protease-activated receptor 1 requires intact caveolin-enriched membrane microdomains in human endothelial cells. *J Thromb Haemost*. 2007;5(12):2437–2444.
47. Awasthi V, Mandal SK, Papanna V, Rao LV, Pendurthi UR. Modulation of tissue factor-factor VIIa signaling by lipid rafts and caveolae. *Arterioscler Thromb Vasc Biol*. 2007;27(6):1447–1455.
48. Zhou R, Tardivel A, Thorens B, Choi I, Tschopp J. Thioredoxin-interacting protein links oxidative stress to inflammasome activation. *Nat Immunol*. 2010;11(2):136–140.
49. Zhou R, Yazdi AS, Menu P, Tschopp J. A role for mitochondria in NLRP3 inflammasome activation. *Nature*. 2011;469(7329):221–225.
50. Miller FJ, et al. Cytokine activation of nuclear factor κ B in vascular smooth muscle cells requires signaling endosomes containing Nox1 and ClC-3. *Circ Res*. 2007;101(7):663–671.
51. Oakley FD, Abbott D, Li Q, Engelhardt JF. Signaling components of redox active endosomes: the redoxosomes. *Antioxid Redox Signal*. 2009;11(6):1313–1333.
52. Juliana C, et al. Anti-inflammatory compounds parthenolide and Bay 11-7082 are direct inhibitors of the inflammasome. *J Biol Chem*. 2010;285(13):9792–9802.
53. Müller M, et al. Localization of tissue factor in actin-filament-rich membrane areas of epithelial cells. *Exp Cell Res*. 1999;248(1):136–147.
54. Ott I, Fischer EG, Miyagi Y, Mueller BM, Ruf W. A role for tissue factor in cell adhesion and migration mediated by interaction with actin binding protein 280. *J Cell Biol*. 1998;140(5):1241–1253.
55. Stossel TP, et al. Filamins as integrators of cell mechanics and signalling. *Nat Rev Mol Cell Biol*. 2001;2(2):138–145.
56. Croall DE, DeMartino GN. Calcium-activated neutral protease (calpain) system: structure, function, and regulation. *Physiol Rev*. 1991;71(3):813–847.
57. Neumar RW, Xu YA, Gada H, Guttmann RP, Siman R. Cross-talk between calpain and caspase proteolytic systems during neuronal apoptosis. *J Biol Chem*. 2003;278(16):14162–14167.
58. Barnoy S, Kosower NS. Caspase-1-induced calpastatin degradation in myoblast differentiation fusion: cross-talk between the caspase calpain systems. *FEBS Lett*. 2003;546(2):213–217.
59. Dalle-Donne I, Giustarini D, Rossi R, Colombo R, Milzani A. Reversible S-glutathionylation of Cys 374 regulates actin filament formation by inducing structural changes in the actin molecule. *Free Radic Biol Med*. 2003;34(1):23–32.
60. Sobierajska K, Skurzynski S, Stasiak M, Kryczka J, Cierniewski CS, Swiatkowska M. Protein disulfide isomerase directly interacts with beta-actin Cys374 and regulates cytoskeleton reorganization. *J Biol Chem*. 2014;289(9):5758–5773.
61. Feng YH, Wang L, Wang Q, Li X, Zeng R, Gorodeski GI. ATP stimulates GRK-3 phosphorylation beta-arrestin-2-dependent internalization of P2X7 receptor. *Am J Physiol Cell Physiol*. 2005;288(6):C1342–C1356.
62. Sorre B, et al. Curvature-driven lipid sorting needs proximity to a demixing point and is aided by proteins. *Proc Natl Acad Sci U S A*. 2009;106(14):5622–5626.
63. Tian A, Capraro BR, Esposito C, Baumgart T. Bending stiffness depends on curvature of ternary lipid mixture tubular membranes. *Biophys J*. 2009;97(6):1636–1646.
64. Sutherland MR, Ruf W, Pryzdial ELG. Tissue factor and glycoprotein C on herpes simplex virus type 1 are protease activated receptor 2 cofactors that enhance infection. *Blood*. 2012;119(15):3638–3645.
65. Svensson KJ, et al. Hypoxia triggers a pro-angiogenic pathway involving cancer cell microvesicles and PAR-2 mediated HB-EGF signaling in endothelial cells. *Proc Natl Acad Sci U S A*. 2011;108(32):13147–13152.
66. Aharon A, Tamari T, Brenner B. Monocyte-derived microparticles and exosomes induce pro-

coagulant and apoptotic effects on endothelial cells. *Thromb Haemost*. 2008;100(5):878–885.
67. Collier ME, Ettelaie C. Induction of endothelial cell proliferation by recombinant and microparticle-tissue factor involves beta1-integrin and extracellular signal regulated kinase activation. *Arterioscler Thromb Vasc Biol*. 2010;30(9):1810–1817.
68. Liang HP, Brophy TM, Hogg PJ. Redox properties of the tissue factor Cys186-Cys209 disulfide bond. *Biochem J*. 2011;437(3):455–460.
69. Wang P, Wu Y, Li X, Ma X, Zhong L. Thioredoxin and thioredoxin reductase control tissue factor activity by thiol redox-dependent mechanism. *J Biol Chem*. 2013;288(5):3346–3358.
70. Ahamed J, et al. Disulfide isomerization switches tissue factor from coagulation to cell signaling. *Proc Natl Acad Sci U S A*. 2006;103(38):13932–13937.
71. Chen VM, Ahamed J, Versteeg HH, Berndt MC, Ruf W, Hogg PJ. Evidence for activation of tissue factor by an allosteric disulfide bond. *Biochemistry*. 2006;45(39):12020–12028.
72. Versteeg HH, Ruf W. Tissue factor coagulant function is enhanced by protein-disulfide isomerase independent of oxidoreductase activity. *J Biol Chem*. 2007;282(35):25416–25424.
73. Butera D, Cook KM, Chiu J, Wong JW, Hogg PJ. Control of blood proteins by functional disulfide bonds. *Blood*. 2014;123(13):2000–2007.
74. Shioji K, Nakamura H, Masutani H, Yodoi J. Redox regulation by thioredoxin in cardiovascular diseases. *Antioxid Redox Signal*. 2003;5(6):795–802.
75. Burke-Gaffney A, Callister ME, Nakamura H. Thioredoxin: friend or foe in human disease? *Trends Pharmacol Sci*. 2005;26(8):398–404.
76. Kishimoto C, Shioji K, Nakamura H, Nakayama Y, Yodoi J, Sasayama S. Serum thioredoxin (TRX) levels in patients with heart failure. *Jpn Circ J*. 2001;65(6):491–494.
77. Ridker PM. Moving beyond JUPITER: will inhibiting inflammation reduce vascular event rates? *Curr Atheroscler Rep*. 2013;15(1):295–0295.
78. Schneider EM, Vorlaender K, Ma X, Du W, Weiss M. Role of ATP in trauma-associated cytokine release and apoptosis by P2X7 ion channel stimulation. *Ann N Y Acad Sci*. 2006;1090:245–252.
79. Wang JG, Manly D, Kirchhofer D, Pawlinski R, Mackman N. Levels of microparticle tissue factor activity correlate with coagulation activation in endotoxemic mice. *J Thromb Haemost*. 2009;7(7):1092–1098.
80. Leaver SK, et al. Increased plasma thioredoxin levels in patients with sepsis: positive association with macrophage migration inhibitory factor. *Intensive Care Med*. 2010;36(2):336–341.
81. Baroja-Mazo A, Pelegrin P. Modulating P2X7 receptor signaling during rheumatoid arthritis: new therapeutic approaches for bisphosphonates. *J Osteoporos*. 2012;2012:408242.
82. Maurice MM, et al. Expression of the thioredoxin-thioredoxin reductase system in the inflamed joints of patients with rheumatoid arthritis. *Arthritis Rheum*. 1999;42(11):2430–2439.
83. Yoshida S, Katoh T, Tetsuka T, Uno K, Matsui N, Okamoto T. Involvement of thioredoxin in rheumatoid arthritis: its costimulatory roles in the TNF-α-induced production of IL-6 and IL-8 from cultured synovial fibroblasts. *J Immunol*. 1999;163(1):351–358.
84. Berckmans RJ, et al. Cell-derived microparticles in synovial fluid from inflamed arthritic joints support coagulation exclusively via a factor VII-dependent mechanism. *Arthritis Rheum*. 2002;46(11):2857–2866.
85. Pawlinski R, et al. Role of cardiac myocyte tissue factor in heart hemostasis. *J Thromb Haemost*. 2007;5(8):1693–1700.
86. Kuida K, et al. Altered cytokine export and apoptosis in mice deficient in interleukin-1 beta converting enzyme. *Science*. 1995;267(5206):2000–2003.
87. Doshi N, Orje JN, Molins B, Smith JW, Mitragotri S, Ruggeri ZM. Platelet mimetic particles for targeting thrombi in flowing blood. *Adv Mater*. 2012;24(28):3864–3869.